

RESEARCH ARTICLE

## Numerical study of convective heat transfer and of turbulent forced of different Nanofluids in channel

Mohammed Bekhti\*<sup>1</sup>, Rachid Saim<sup>1</sup>

<sup>1</sup>Applied Energy and Thermal Laboratory (ETAP), Department of Mechanical Engineering, Faculty of Technology, Abou Bekr Belkaid University. Tlemcen, B.P 230, Chetouane, Tlemcen, 13000, Algeria

Corresponding Author: Mohammed Bekhti, engr.osmangoni@yahoo.com

Received: 25 December, 2022, Accepted: 14 January, 2022, Published: 10 January, 2022

### Abstract

In this study, the flow field and heat transfer of different nanofluids (AL<sub>2</sub>O<sub>3</sub>, CuO, SiO<sub>2</sub>, ZnO), turbulent forced convection in a channel. The surface of the channel is hot  $T_h = 310$  K. Simulations are carried out for constant water Prandtl number of 6.99, Reynolds numbers from 20,000, 30,000, 40,000, 50,000 to 60,000, nanoparticles volume fractions of 0, 0.01, 0.02, 0.03, 0.04 and nanoparticles diameter of 30 nm. The finite volume method and SIMPLE algorithm and k- $\epsilon$  are utilized to solve the governing equations numerically. The numerical results showed that with enhancing Reynolds numbers and volume fractions, average Nusselt number increases.

**Keywords:** Nanofluid; channel; Turbulent flow; Forced convection; Nusselt number; Numerical solution; Reynolds numbers

### Introduction

Turbulent flow in the channels is the subject of importance in many engineering applications and of interest to many researchers. Some of them include energy conversion systems found in the same nuclear reactor design, heat exchangers, solar collectors, and cooling of industrial machinery and electronic components. Of great importance for the innovation of these studies in addition to experimental and numerical techniques is the research on the flow and heat transfer processes for the improvement of heat exchangers. Large-scale experimental studies of turbulent flow, heat transfer and heat exchangers have been carried out by various authors. The digital study by DIAO XU et al [1] is based on the Computational Fluid Dynamic method for improving the performance of nanofluid flows and heat transfer in micro channels. It has been found that nanoparticles improve the heat transfer of fluids by a certain percentage, and cause a sharp increase in viscous shear stress on the wall, which leads to an increase in the power to pass nanofluids into the wall. the canal. Adnan M Hussein et al [2] with the aim of improving convective turbulent heat transfer and studied numerically the flow of the heated tube using TiO<sub>2</sub>-water nanofluid, was used to predict the friction factor and the Nusselt number for heat transfer by forced convection of the TiO<sub>2</sub>-water nanofluid. The Reynolds number range is 10,000 to 100,000 to be turbulent flow in a horizontal straight tube with a heat flow of 5,000 w / m<sup>2</sup>. Azher M et al [3] studied numerically from a turbulent flow fully developed heat transfer behavior in trapezoidal channel systems, when using several types of nanoparticles (Al<sub>2</sub>O<sub>3</sub>, CuO, SiO<sub>2</sub>, ZnO), with different

volume fractions (0% to 4%), and diameter (20nm-80nm) and a heat constant of 6kw / m<sup>2</sup>; the results indicate that SiO<sub>2</sub> has the highest Nusselt number compared to the others. To improve heat transfer, it is a matter of increasing the volume concentration of nanoparticles and reducing the diameter if the pressure drops increase. Ajay Singh et al [4] studied numerically was carried out to observe the effect of the nanofluid on the characteristics of heat transfer by convection in the developing region of the flow of the tube, the average particle size varies from  $d_p = 15$  at 150 nm and a particle concentration of 1, 2, 4, 6 and 10% were used in this work. The single-phase method with constant heat flow to the wall was used for the analysis. Jubair A. Shamim et al [5] numerically evaluated computational fluid dynamics (CFD) is performed to determine the thermo- and hydrodynamic performance of the water-alumina (Al<sub>2</sub>O<sub>3</sub>) nanofluid in a square subchannel exhibiting ratios pitch-diameter of 1.25 and 1.35 Two fundamental aspects of thermal hydraulics. Heat transfer and pressure drop are evaluated under typical pressurized water reactor (PWR) conditions at different flow rates ( $300,000 < Re < 600,000$ ) using pure water and different concentrations of water-alumina nanofluid (0.5–3.0 vol. %) as coolant. The experimental study led by M. Siva Eswara Rao et al [6] using nanoparticles with a diameter of 28 nm (Al<sub>2</sub>O<sub>3</sub>) with different volume concentrations (0.1%, 0.2%, 0.3%, 0.4%) in a tube with several exchanger passes heat transfer coefficient to improve the heat transfer coefficient by forced convection under turbulent flow conditions, the inlet and outlet temperature are measured and the nanofluid volume fraction concentration is tested with the same temperature and speed. If we add the nanoparticles

in the base fluid, we improve the heat transfer and we increase the conductivity, density, thermal diffusivity and friction factor. AV Minakov et al [7] have experimented with the forced (turbulent) convection of nanofluids in cylindrical and spherical cavity channels, with nanoparticles of zirconium oxide (ZrO<sub>2</sub>) of average size of 44 and 105, the Reynolds number varying from 3000-8000. Note that the increase in heat transfer coefficient and pressure drop, that the use of nanofluids depends on the shape of the channel surface. The object of the study by Sami D. Salman et al [8] was improved heat transfer rate compared to individual uses of ribs or nanofluids. The main objective of the present research is to study the combined effects of various programs of the types of nanofluids ZnO, CuO, Al<sub>2</sub>O<sub>3</sub> and SiO<sub>2</sub> with various volume fractions (1% -4%) and different sizes of nanoparticles (dp = 30 nm, 40 nm, 50 nm and 60 nm) in a constant thermal flux tube with rectangular, triangular and trapezoidal ribbed by ANSYS-FLUENT version 16 software using the standard model k-ε. So using nanofluids with different ribbed tube configurations is the most effective technique. For the other application improves heat transfer rate compared to individual use of ribs or nanofluids. Hamdi E et al [9] launches a digital study of the turbulent flow of nanofluids in a triangular rib duct, nanoparticles (Al<sub>2</sub>O<sub>3</sub>, SiO<sub>2</sub>) with EG base fluid (Ethylene Glycol) are used, the volume concentration varies from 1% up to 'at 6%, the Reynolds number is 4000-32000. The results in the case of SiO<sub>2</sub>-EG are 6% of the volume, Re = 32000, the Nusselt number is higher compared to the number of Re = 4000. So if we increase the concentration of nanoparticles, we notice an increase in the coefficient of friction. Mohammad Hemmat Esfe et al [10] This article reviews and summarizes the application of fluids and nanofluids in photovoltaic thermal systems (PVT). Numerical, analytical and experimental literatures are studied. PVT introduced as a combined version of solar collectors and photovoltaic

technology to achieve simultaneous generation of thermal and electric energy is a combination of photovoltaic and solar collector technology in a system that simultaneously generates electric and thermal energy. The application of fluids and nanofluids in PVTs was evaluated by a study of single fluid flows, dual fluid (air-liquid) flows, phase change materials (PCM) and nanofluid flows. The aim of this work is Numerical study of the turbulent flow field of different nanofluids (AL<sub>2</sub>O<sub>3</sub>, CuO, SiO<sub>2</sub>, ZnO), through a tube, the heat flow constant and uniform at the walls. The analysis of the turbulent nanofluid flow in this tube allows understanding the thermal behaviour in different nanoparticle concentrations. The improvement of the heat transfer increases with the volume concentration of the particles and the Reynolds number and the comparisons with the correlations. The results of the simulation are then analysed to explain the thermal phenomena occurring in the system.

**The schematic of geometry studied:**

A numerical simulation of heat transfer by forced convection in a channel is considered in 2 dimensions where the geometry is shown in figure 1. The configuration of the simulation via fluent 6.3.26 involves a channel with a length of 0.5 m and with a diameter of 0.02 m while the wall channel exhibiting a constant temperature of 310 K. The initial condition and at the limits of the simulation, the temperature of the nanofluids will be set at an initial value of 300 K at the inlet. The parameters studied varied with each simulation adopting a Reynolds number of 20,000 and 60,000 and at a variable volume fraction of 1 - 4%. In this study, the simulated nanofluids are assumed to be incompressible, single-phase, exhibiting a stable and turbulent flow with constant thermophysical properties.

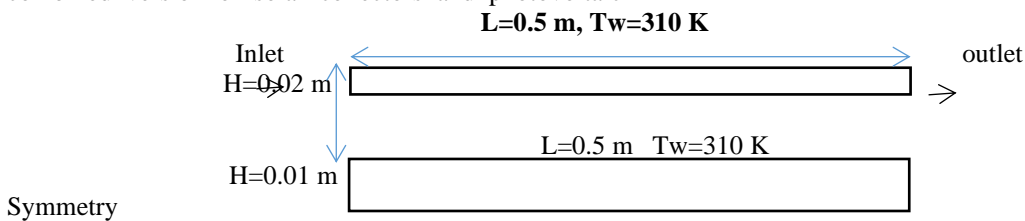


Fig. 1. Geometry of the channel model.

**The governing equations**

**Continuity equation:**

$$\frac{\partial}{\partial x_i} (\rho u_i) = 0$$

**Momentum equation:**

$$\frac{\partial}{\partial x_i} (\rho u_i u_j) = -\frac{\partial p}{\partial x_i} + \frac{\partial}{\partial x_j} \left[ \mu \left( \frac{\partial u_i}{\partial x_j} + \frac{\partial u_j}{\partial x_i} \right) \right] + \frac{\partial}{\partial x_j} (-\overline{\rho u'_i u'_j})$$

**Energy equation:**

$$\frac{\partial}{\partial x_i} (\rho u_i T) = \frac{\partial}{\partial x_j} [(\Gamma + \Gamma_t) \frac{\partial T}{\partial x_j}]$$

Where  $\mu$  and  $\mu_t$  are the molecular viscosity and the vortex viscosity, respectively.

**Turbulence Model**

The turbulence model selected in the simulations is the standard k-ε turbulence model with its associated enhanced near-wall function enabled with the software running simulation.

The standard k-ε turbulence model in two ways of formulation regarding turbulent viscosity and dissipation rate ε transport equation.

**Turbulent kinetic energy equation k-ε:**

$$\frac{\partial}{\partial x_j}(\rho k u_j) + \frac{\partial}{\partial t}(\rho k) = \frac{\partial k}{\partial x_j} \left( \mu + \frac{\mu_t}{\sigma_k} \right) + G_k + S_k - \rho \epsilon$$

Where  $G_k$  is the generation of kinetic turbulence energy due to average velocity gradients and it is expressed as

$$G_k = (-\rho \overline{u_i u_j}) \frac{\partial u_j}{\partial x_i}$$

And based on the Boussines hypothesis,  $G_k$  is defined as

$$G_k = \mu_t s^2$$

The rate of dissipation of turbulent kinetic energy ε is defined as follows:

$$\frac{\partial}{\partial t}(\rho \epsilon) + \frac{\partial}{\partial x_j}(\rho \epsilon u_j) = \frac{\partial \epsilon}{\partial x_j} \left( \frac{\partial}{\partial x_j} \left( \mu + \frac{\mu_t}{\sigma_\epsilon} \right) \right) + \rho \left( C_1 s \epsilon - C_2 \frac{\epsilon^2}{k + \sqrt{v \epsilon}} \right) + s \epsilon$$

The values of the constants in the above equations:

$$C_1 = 1.44, C_2 = 1.9, \sigma_\epsilon = 1.2$$

$$C_\mu = \max\left(0.43, \frac{\eta}{\eta + 5}\right)$$

$$\eta = s \frac{k}{\epsilon}$$

$$s = \sqrt{2(s_{ij})^2}$$

$$\mu_t = \rho C_\mu \frac{k^2}{\epsilon}$$

$$C_\mu = \frac{1}{A_0 + A_s \frac{k u^*}{\epsilon}}$$

**Numerical procedure**

The governing equations with the connected boundary conditions are numerically solved using the finite volume method. The thermophysical properties like thermal conductivity and viscosity, which are variable with temperature, are solved concurrently with flow,

temperature in the whole solution domain. On the control volume faces these properties are averaged the calculated values on the grids. The SIMPLE algorithm has been adopted to solve for the pressure and the velocity components. The coupled sets of discretized equations have been solved iteratively using a line-by-line procedure. Table 1: Thermophysical properties of the base fluid and the nanoparticles used in this study [11, 12, 13 and 14]:

| property                        | Pure water | AL2O3 | CuO   | SiO2 | ZnO   |
|---------------------------------|------------|-------|-------|------|-------|
| Density<br>ρ (kg/m3)            | 998        | 3970  | 6500  | 2200 | 5600  |
| Specific heat<br>Cp (j/kg.k)    | 4182       | 765   | 535.6 | 703  | 495.2 |
| Thermal conductivi<br>K (w/m.k) | 0.597      | 40    | 20    | 1.2  | 13    |
| Dynamic viscosity<br>μ (Ns/m2)  | 0.000998   | -     | -     | -    | -     |

**Mesh independent test**

In the present study, I chose the size of the grid near the boundary layer flow channel wall near the wall at Reynolds number  $Re = 40,000$ . I do the network independence tests that were performed to assess the

effects of grid sizes on maximum temperature, outlet velocity and maximum fluid along the channel. Four mesh sets were generated with the node numbers 200x40, 212x42, 218x43, 220x43; 225x45 and 250x50, respectively. It has been noticed that the Nusselt number

of 218x43 nodes gives closer and acceptable results to validate the results, was selected to save computation time. The different grids, Re = 40,000.

| Mesh   | T max    | V outlet | V max  |
|--------|----------|----------|--------|
| 200x40 | 309,8311 | 1,1074   | 2,2706 |
| 212x42 | 309,8943 | 1,0678   | 2,2631 |
| 218x43 | 309,9164 | 1,0483   | 2,2594 |
| 220x43 | 309,9164 | 1,0483   | 2,2594 |
| 225x45 | 309,9476 | 1,0101   | 2,2521 |
| 250x50 | 309,9835 | 0,9198   | 2,2345 |

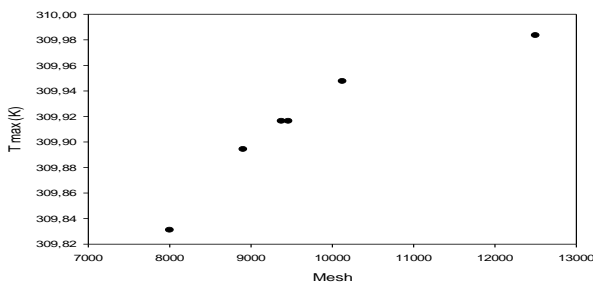


Fig. 2. Grid independence test Maximum temperature

### Validation

The simulations were carried out using the FLUENT 6.3.26 software. A finite volume process was used to numerically solve the continuity, momentum and energy equations using the turbulence model. The standard k-ε model with SIMPLE algorithm was selected for the simulation. The convergence criterion is considered to be 10<sup>-6</sup> for all the variables.

In order to validate the numerical procedure, the relations presented with Gnielinski [15], Pak and Cho [16], Maiga al. [17] and Dittus boelter correlation [18]. The results are compared with the existing results in the literature.

Gnielinski [15]:  

$$Nu = 0.012 (Re^{0.87} - 280) Pr^{0.4} \quad 1.5 \leq Pr \leq 500, 3 \cdot 10^3 \leq Pr \leq 10^6 \quad (19)$$

Pak & Cho [16]:  

$$Nu = 0.021 Re^{0.8} Pr^{0.5} \quad (20)$$

Maiga & al. [17]:

$$Nu = 0.085 Re^{0.71} Pr^{0.35} \quad (21)$$

Dittus boelter correlation [18]  

$$Nu = 0.023 Re^{0.8} Pr^{0.4}$$

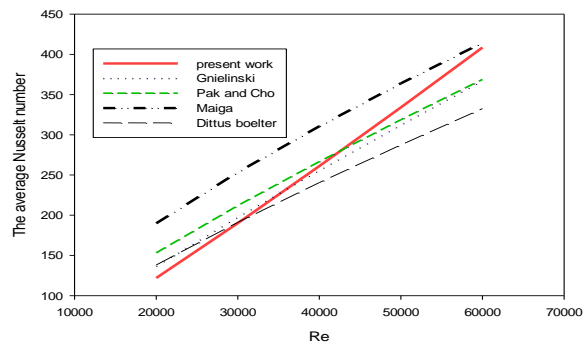


Fig.3. Comparison of the present results with equations of Gnielinski [15], Pak and Cho [16], Maiga al. [17] and Dittus boelter correlation [18].

### The equations considers for evaluates nanofluids

The following formulas are used to determine properties such as density, specific heat, dynamic viscosity, and thermal conductivity (Eq; 1, 2, 3.4) of the nanofluid.

Density:

The density of the nanofluid is given as [19]:

$$\rho_{nf} = (1 - \varphi)\rho_{bf} + \varphi\rho_p \quad (1)$$

Where  $\rho_f$  and  $\rho_{np}$  are the density of the based fluid and the solid nanoparticles, respectively.

Heat capacity:

The heat capacity of the nanofluid is expressed as [20]:

$$Cp_{nf} = (1 - \varphi)Cp_{bf} + \varphi Cp_p \quad (2)$$

Where  $(\rho Cp)$  and  $(\rho Cp)$  are the heat capacity of the based fluid and the solid nanoparticles, respectively.

Dynamic viscosity:

The effective dynamic viscosity of the nanofluid is given as [21]:

$$\mu_{nf} = \mu_{bf} * \frac{1}{(1 - 34.87 * (d_p/d_f)^{-0.3} * \varphi^{1.03})} \quad (3)$$

$$d_f = \left[ \frac{6 * M}{N * \pi * \rho_{bf}} \right]$$

Where  $M$  is the molecular weight of the base fluid,  $N$  is the Avogadro number = 6.022 × 10<sup>23</sup> mol<sup>-1</sup>, and  $\rho_f$  is the

mass density of the base fluid calculated at temperature  $T_0 = 300\text{K}$ . It could be noticed that, for simplicity in this study, the changes of viscosity with temperature along the channel and the viscosity at all points is considered to be the same as the viscosity at inlet temperature

**Thermal conductivity**

The effective thermal conductivity of the nanofluid is given as [22]:

By considering Brownian motion of nanoparticles in channel, the effective thermal conductivity can be obtained by using the mean empirical equations:

$$k_{\text{eff}} = k_{\text{static}} + k_{\text{brownian}} \quad (4)$$

Where  $k_{\text{static}}$  indicates the thermal conductivity improvement from the advanced thermal conductivity of nanoparticles and  $k_{\text{Brownian}}$  represents the effect of Brownian motion of particles.  $k_{\text{Brownian}}$  has also considered the influence of movement of fluid particles with nanoparticles. Consider the following:

$$k_{\text{static}} = k_{\text{bf}} \left[ \frac{(k_p + 2k_{\text{bf}}) - 2\varphi(k_{\text{bf}} - k_p)}{(k_p + 2k_{\text{bf}}) + \varphi(k_{\text{bf}} + k_p)} \right]$$

Where  $k_s$  and  $k_f$  are thermal conductivities of the nanoparticles and the base fluid, respectively. Consider the following:

$$k_{\text{brownian}} = 5 * 10^4 \beta \varphi \rho_{\text{bf}} C_{p_{\text{bf}}} \sqrt{\frac{K_B T}{2 \rho_p d_p}} f(T, \varphi)$$

where  $\rho_f$  and  $\rho_s$  are the densities of the base fluid and the particles, respectively, and  $C_{p,f}$  is the specific heat capacity of the base fluid.  $K_B$  is the Boltzmann constant,  $1.381 \times 10^{-23} \text{ J/k}$ .  $\beta$  is a parameter which indicates the effect of interaction between nanoparticles and the movement of fluid around the particles.  $f(T, 0)$  represents the temperature dependency of nanofluids, where both ( $T$ ), and  $\beta$  were obtained by utilizing the existing experimental data. The modified ( $T$ ), equation was reported by Vajjha and Das [22]:

$$f(T, \varphi) = (2.8217 * 10^{-2} \varphi + 3.917 * 10^{-3}) \left( \frac{T}{273.15} \right) + (-3.0669 * 10^{-2} \varphi - 3.91123 * 10^{-3})$$

The values of  $\beta$  for different nanoparticle types [23, 24]:

| Type particle | $\beta$                     | Concentration (%)            | Température (K)                       |
|---------------|-----------------------------|------------------------------|---------------------------------------|
| Al2O3         | $8.4407(100\varphi)^{-1}$   | $1\% \leq \varphi \leq 10\%$ | $298\text{K} \leq T \leq 363\text{K}$ |
| CuO           | $9.881(100\varphi)^{-0.94}$ | $1\% \leq \varphi \leq 6\%$  | $298\text{K} \leq T \leq 363\text{K}$ |

|      |                           |                              |                                       |
|------|---------------------------|------------------------------|---------------------------------------|
| SiO2 | $1.9526(100\varphi)^{-1}$ | $1\% \leq \varphi \leq 10\%$ | $298\text{K} \leq T \leq 363\text{K}$ |
| ZnO  | $8.4407(100\varphi)^{-1}$ | $1\% \leq \varphi \leq 7\%$  | $298\text{K} \leq T \leq 363\text{K}$ |

**Calcul of  $\beta$  for different nanoparticle types**

|       | $\beta$ 1% | $\beta$ 2% | $\beta$ 3% | $\beta$ 4% |
|-------|------------|------------|------------|------------|
| AL2O3 | 0,713409   | 4,012003   | 2,596619   | 1,906971   |
| CuO   | 9,881      | 5,133907   | 3,500356   | 2,667442   |
| SiO2  | 1,9526     | 0,710052   | 0,392919   | 0,258206   |
| ZnO2  | 8,4407     | 4,012003   | 2,596619   | 1,906971   |

**Results and discussion**

To study the effect of the volume fraction of different nanoparticles (AL2O3, CuO, SiO2, ZnO), on the mean Nusselt number. Here, the effect of the volume fraction of nanoparticles on the mean Nusselt number is presented for  $d_p = 30 \text{ nm}$ . Figures (4, 5, 6, 7) shows the variations of the mean Nusselt number as a function of the Reynolds number for different volume fractions. For all the volume fractions studied, the mean Nusselt number increases with the increase in the Reynolds number. This is acceptable due to the increase in the conductivity of the nanofluid and the subsequent improvement in heat transfer. The other reason for this increase in the mean Nusselt number is the acceleration of energy transport due to the random motion of nanoparticles (Brownian motion) inside the nanofluid. This process allows a more uniform temperature distribution inside the nanofluid and therefore an improved heat transfer rate between the nanofluid and the wall.

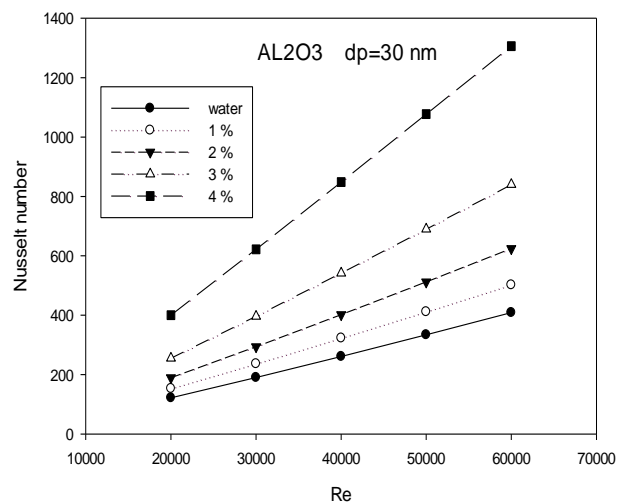


Fig.4. The effect of different concentrations of volume nanoparticles AL2O3 at different Reynolds numbers on the Nusselt number

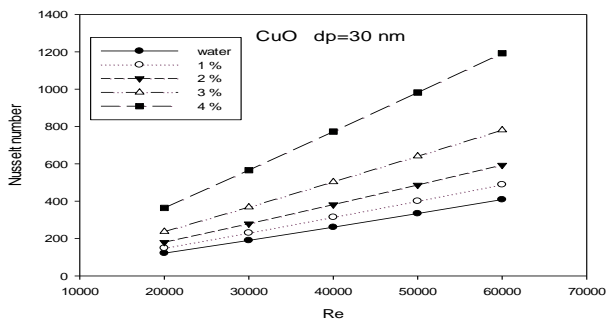


Fig.5. The effect of different concentrations of volume nanoparticles CuO at different Reynolds numbers on the Nusselt number

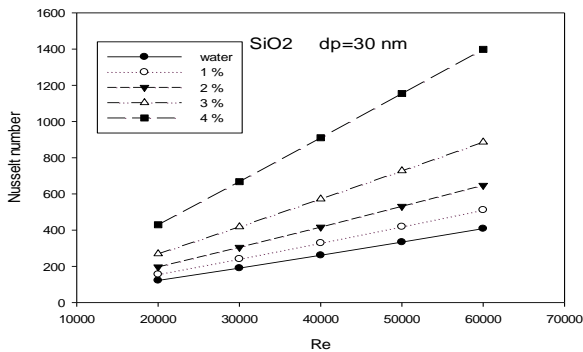


Fig.6. The effect of different concentrations of volume nanoparticles SiO2 at different Reynolds numbers on the Nusselt number

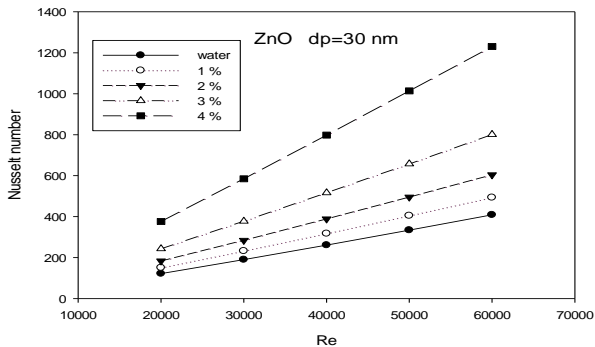


Fig.7. The effect of different concentrations of volume nanoparticles ZnO at different Reynolds numbers on the Nusselt number

The most increment in the average Nusselt number for a fixed volume fraction of 0.01 in figure 8, where the average Nusselt number rises up and for an increment in Reynolds number from 20,000 to 60,000.

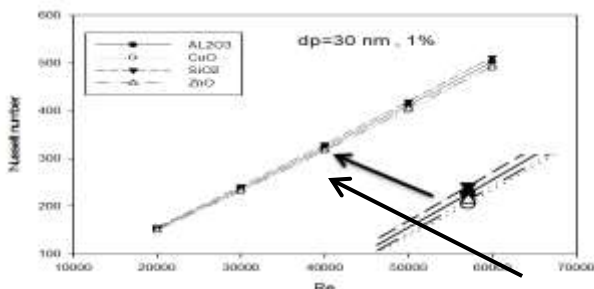


Fig.8. The effect 1% of different nanofluid at different Reynolds numbers on the Nusselt number.

The most increment in the average Nusselt number for a fixed volume fraction takes place in volume fraction of 0.04 in figure 9, where the average Nusselt number rises up and for an increment in Reynolds number from 20,000 to 60,000.

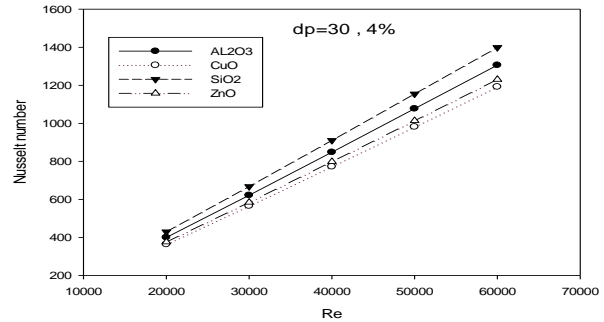


Fig.9. The effect 4% of different nanofluid at different Reynolds numbers on the Nusselt number.

With an increasing volume fraction ranging from 0.01 to 0.04 for a fixed Reynolds number  $Re = 40,000$ , the average Nusselt number increases for nanoparticles figure 10. The mean values of the Nusselt number for the SiO2 nanoparticle differ from other nanoparticles.

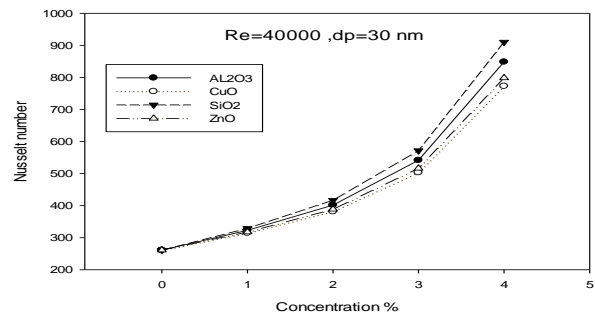


Fig.10. The effect the Reynold number  $Re=40000$  on of different nanofluid at different concentrations of volume nanoparticles on the Nusselt number.

### Conclusions

In this study, the forced convection heat transfer of different nanofluids inside a symmetrical channel for Reynolds numbers from 20,000 to 60,000, volume fractions of nanoparticles in a range of 0.01 to 0, 04 and a diameter of 30 nm was considered. The channel wall is maintained at 310 K and the input nanofluid flux is at 300 K. Based on the numerical results.

For all the studied volume fractions, the average Nusselt number increases with increasing Reynolds number. with increasing the reynolds number 20.000 to 60.000 and changed the volume friction up the 0.01 to 0.04 the average Nusselt number the pure water and nanofluid increases. The most increment in the average Nusselt number for a fixed volume fraction takes place in volume fraction of 0.04, where the average Nusselt number rises up to for an increment in Reynolds number from 20,000 to 60,000.

## Nomenclature

### Symbols:

P pressure, Pa  
T Temperature, K  
H channel height, m  
 $\Gamma$  thermal diffusivity,  $m^2.s^{-1}$   
 $\Gamma_t$  turbulent diffusivity, (...)  
k turbulent kinetic energy,  $m^2.s^{-2}$   
q heat flux,  $kw.m^{-2}$   
h heat transfer coefficient,  $w.m^{-2}.K^{-1}$   
fr friction factor, (...)  
L length, m  
u speed,  $m.s^{-1}$   
Re Reynolds number, (...)  
Pr Prandtl number, (...)  
Nu Nusselt number, (...)  
U input speed,  $m.s^{-1}$

### Greek letters:

$\rho$  density,  $kg.m^{-3}$   
 $\lambda$  thermal conductivity,  $W.m^{-2}.K^{-1}$   
 $\mu$  dynamic viscosity,  $kg.m^{-1}.s^{-1}$   
Cp specific heat kj  
 $\alpha_k$  effective dissipation Prandtl number,  
 $\mu_{eff}$  effective dynamic viscosity,  
 $\varepsilon$  dissipation kinetic energy,  $m^2.s^{-3}$   
 $\phi$  Particle concentration  
C1 Constant used in the standard  $k-\varepsilon$  model  
C2 Constant used in the standard  $k-\varepsilon$  model  
C $\mu$  Constant used in the standard  $k-\varepsilon$

### Index :

W wall,  
t turbulent,  
eff effective  
nf nano fluid  
np nano particle  
p particle  
f base fluid

## References

- DIAO XU, LUNSHENG PAN, Numerical study of nanofluid flow and heat transfer in micro-channels, *International Journal of Nanoscience*, Vol. 5, No. 6 (2006) 747-752.
- Adnan M Hussein, RA Bakar, K Kadirgama and KV Sharma, Simulation study of turbulent convective heat transfer enhancement in heated tube flow using TiO<sub>2</sub> -water nanofluid, *Materials Science and Engineering* 50 (2013) 012035, doi: 10.1088 / 1757-899X / 50/1/012035.
- Azher M. Abed M.A. Alghoul K. Sopian H.A. Mohammed Hasan sh. Majdi Ali Najah SAl-. Shamani, Design Features of Corrugated Trapezoidal Plate Heat Exchangers Using Nanofluids, *Chemical Engineering and Processing* <http://dx.doi.org/10.1016/j.cep.2014.11.005>.
- Ajay Singh, Bireswar Paul, Numerical Study of Convection Heat Transfer using Nanofluid in the Developing Region of a Tube Flow, *Journal of Advances in Mechanical Engineering and Science (JAMES)*, DOI: 10.18831 / james.in / 2015031002.
- Jubair A. Shamim, Palash K. Bhowmik, Chen Xiangyi, Kune Y. Suh, A new correlation for convective heat transfer coefficient of water – alumina nanofluid in a square array subchannel under PWR condition, *Nuclear Engineering and Design* 308 (2016 ) 194–204.
- M. Siva Eswara Rao, Dowluru Sreeramulu, C.J. Raoc, M.V. Ramana, Experimental study on the coefficient of heat transfer by forced convection of a nanofluid, *Materials Today: Proceedings* 4 (2017) 8717–8723.
- A.V. Minakov, D.V. Guzei, K.N. Meshkov, I.A. Popov, A.V. Shchelchkov, Experimental study of the turbulent forced convection of nanofluids in channels with cylindrical and spherical cavities, *International Journal of Heat and Mass Transfer* 115 (2017) 915–925.
- Sami D. Salman, comparative study on heat transfer by improving the flow of nanofluids in the finned tube and using CFD simulation. *Heat Transfer-Asian Res.* 2018; 1–16. DOI: 10.1002 / htj.21376
- Hamdi E. Ahmed, BH Salman, A. Sh. Kerbeet, Improvement of the heat transfer of a forced turbulent flow of nanofluids in a duct using a triangular rib, *International Journal of Heat and Mass Transfer* 134 (2019) 30 –40.
- Mohammad Hemmat Esfe, Mohammad HassanKamyab, MajidValadkhani, Application of nanofluids and fluids in photovoltaic thermal system: An updated review, *Solar Energy* Volume 199, 15 March 2020, Pages 796-818, <https://doi.org/10.1016/j.solener.2020.01.015>.
- Oronzio Manca, Sergio Nardini, Daniele Ricci, A numerical study of nanofluid forced convection in ribbed channels, *Applied Thermal Engineering* 37 (2012) 280-292.
- R. S. Vajjha and D. K. Das, “Experimental determination of thermal conductivity of three nanofluids and development of new correlations,” *International Journal of Heat and Mass Transfer*, vol. 52, no. 21-22, pp. 4675–4682, 2009.
- R. S.Vajjha, D. K. Das, andD.P.Kulkarni, “Development of new correlations for convective heat transfer and friction factor in turbulent regime for nanofluids,” *International Journal of Heat and Mass Transfer*, vol. 53, no. 21-22, pp. 4607–4618, 2010.

- J. H. Lienhard and J. Lienhard, *A Heat Transfer Textbook*, Phlogiston Press, Cambridge, Mass, USA, 2000.
- [15] A. Bejan, *Heat Transfer*, John Wiley & Sons, New Jersey, 1993.
- B. C. Pak and Y. I. Cho, "Hydrodynamic and heat transfer study of dispersed fluids with submicron metallic oxide particles," *Experimental Heat Transfer*, vol. 11, no. 2, pp. 151–170, 1998.
- S. E. B.Ma'iga,C.T.Nguyen, N. Galanis, G. Roy, T.Mar' e, andM.Coqueux, "Heat transfer enhancement in turbulent tube flow using Al<sub>2</sub>O<sub>3</sub> nanoparticle suspension," *International Journal of Numerical Methods for Heat and Fluid Flow*, vol. 16, no. 3, pp. 275–292, 2006.
- F. W. Dittus and L. M. K. Boelter, *Heat Transfer for Automobile Radiators of the Tubular Type*, vol. 2 of *University of California Publications in Engineering*,University of California Press, 1930.
- B. C. Pak, Y.I. Cho, Hydrodynamic and heat transfer study of dispersed fluids with submicron metallic oxide particles, *Experimental Heat Transfer an International Journal*, 11 (1998), 151-170.
- Y. Xuan, W. Roetzel, Conceptions for heat transfer correlation of nanofluids, *International Journal of Heat and Mass Transfer*, 43 (2000), 3701-3707.
- M. Corcione, Empirical correlating equations for predicting the effective thermal conductivity and dynamic viscosity of nanofluids, *Energy Conversion and Management*, 52 (2011), 789-793.
- R.S. Vajjha, D.K. Das, A review and analysis on influence of temperature and concentration of nanofluids on thermophysical properties, heat transfer and pumping power. *International Journal of Heat and Mass Transfer*, 55 (2012) 4063-4078.
- R.S. Vajjha, D.K. Das, Experimental determination of thermal conductivity of three nanofluids and development of new correlations, *Int. J. Heat Mass Transf.* 52 (21-22) (2009) 4675–4682.
- R.S. Vajjha, D.K. Das, D.P. Kulkarni, Development of new correlations for convective heat transfer and friction factor in turbulent regime for nanofluids, *Int. J. Heat Mass Transf.* 53 (21) (2010) 4607–4618.